JET–P(99)61

F Rochard et al

Characteristics of Internal Transport Barriers from the JET Optimised Shear Database

JET–P(99)61

Characteristics of Internal Transport Barriers from the JET Optimised Shear Database

F Rochard[1], X Litaudon[1], F X Söldner, Yu F Baranov,
G D Conway, C Gormezano, A C C Sips.

JET Joint Undertaking, Abingdon, Oxfordshire, OX14 3EA,
[1]Association Euratom-CEA, Département de Recherches sur la Fusion Contrôlée,
Centre d'Etudes de Cadarache, F-13108 Saint-Paul-Lez-Durance Cedex, France.

Preprint of a Paper to be submitted for publication in Nuclear Fusion

February 2000

ABSTRACT

The general features of the Internal Transport Barriers (ITBs) obtained in the JET "Optimised Shear" regime are deduced from the analyses of a large database of discharges including the experiments performed with a mixture of Deuterium-Tritium (D-T) ions. The coupled and complex spatio-temporal dynamics of the ITBs are studied from the radial profiles measurements of the thermal ion and electron temperatures. The spatial locations of the ITBs inside the plasma column are deduced from the radial derivatives of the plasmas profiles. In particular, our analyses show that the radial positions of the ITB follow the same evolution for both the electron and ion temperature profiles.

Among the JET "Optimised Shear" database, we propose to distinguish two categories of discharges depending on the edge conditions: the ITBs are triggered either with an L-mode edge or simultaneously with an edge transport barrier (H-mode). The characteristics of the ITBs and plasma performances of these two categories are compared. Experimental conditions to successfully combine the edge and core transport barriers are given. In particular, emphasis is given on the description and analyses of the "Optimised Shear" discharges which combine an ITB with an ELMy edge since this operating mode opens the route to high performance regimes which could be extrapolated towards steady-state conditions.

1. INTRODUCTION

Improvement of the tokamak concept in terms of stability and confinement has received an increasing interest in fusion research in view of achieving high-performance and steady-state operation (e.g. [1-3]). Higher confinement plasma properties with respect to standard L-mode scaling appear promising for increasing fusion performance and the self-generated bootstrap current required for fully non-inductive regime. In addition to the improved confinement regime with a transport barrier located at the plasma edge (H-mode), it has been shown that manipulation of the current and pressure profiles could also lead to the reduction of the anomalous transport inside the plasma core: formation of an Internal Transport Barrier (ITB). As previously suggested by theoretical analyses (e.g. [4]), high core pressure with reduced transport coefficients could be sustained in plasma regions characterised by broad or hollow current density profiles associated with a weak or negative magnetic shear, s ($s = r/q(dq/dr)$ where q is the safety factor, and r the radius of the magnetic surface). On the experimental side, internal transport barriers have been obtained in most tokamaks (ASDEX-Upgrade [5], DIII-D [6], FTU [7], JET [8], JT60-U [9-10], RTP [11], TFTR [12], Tore Supra [13-14]) by shaping the q-profiles during the current ramp-up phase of the discharge while heating the plasma to delay the natural penetration of the off-axis ohmic current towards the plasma centre. Using this approach, high performance plasmas with high fusion yield production both in D-D and D-T plasmas have been obtained on JET in the so-called "Optimised Shear" regime [15-17]. In addition to these operating modes transient by nature, it is worth mentioning that hollow current density profiles have also been sustained in

steady-state condition but at reduced performance by generating off-axis non-inductive lower hybrid current drive [18-20].

This paper reports the analyses of the large database of "Optimised Shear" discharges obtained during the 1996-1997 experimental campaign at JET including both the D-D and D-T operation [21-22]. Experiments were performed in a lower single null X-point magnetic configuration with the so-called " Mark IIA " divertor at a toroidal magnetic field ranging from 3.4T up to 3.8T. The aim of this work is to characterise the performances of the "Optimised Shear" regime on a more statistical basis, i.e. without selecting a reduced subset of high performance plasma discharges. Indeed, the general trends and characteristics of this relatively new operating mode at JET are inferred from the analysis of database containing up to 300 pulses with ITBs. In this database, the plasmas discharges are characterised with both the global (i.e., volume integrated) and local (i.e., information on the radial profiles) quantities.

In this present work, we propose to classify the JET "Optimised Shear" discharges into two categories. In the first class of discharges, ITBs are triggered while keeping an L-mode edge. In such conditions, the highest neutron rates in D-D plasmas have been obtained in JET up to 5.610^{16} neutron/s [15] and in D-T plasmas the fusion power has reached up to 8.2MW [16]. Nevertheless, it appears that the high reactivity plasmas are difficult to sustain during more than few confinement times due to the final and inevitable transition from an L-mode edge to an ELM-free H-mode (ELM stands for Edge Localised Mode). The continuous build-up of pressure at the edge usually leads to the disruptive termination of the ELM-free H-mode phase and the lost of the plasma performances. In the second class of discharges, ITBs are triggered simultaneously with an ELMy H-mode edge where the regular ELMs avoid the pressure build-up at the plasma edge. Therefore ITB discharges with an ELMy edge have promising potential for achieving high performance operation in steady conditions, i.e. where high confinement properties have been sustained for several energy confinement times [23]. The conditions to successfully sustain this "Double Barrier" mode as called in reference [23] are discussed together with the comparison of the ITB's characteristics obtained with different edge conditions.

The paper is divided in four main parts. After this introduction, a brief description of the operational scenario used to produce the internal transport barriers in JET is given in section two. It will be shown in this part that a minimum additional power is required to trigger an ITB. The method used to numerically locate the radial position of the ITBs is detailed in section 3. The radial location and time evolution of the ITBs for both the electron and ion temperatures profiles are presented in this part together with a discussion on the links between their radial location and the global energy confinement. Then, section four deals with the requirements on the q-profile shapes to trigger an ITB in addition to the necessary additional power previously discussed. Emphasis is given on the role played by the weak magnetic shear inside the rational q-surfaces (i.e. q=2) to trigger an ITB. Before summarising our results in the conclusion, section five describes the operating domain and constrain required to successfully combine an internal

transport barrier with an edge transport barrier in view of approaching steady-state operation together with high-performances.

2. DESCRIPTION OF THE OPERATIONAL SCENARIO

To trigger a core transport barrier in a reliable manner, an operational scenario has been fully defined and regularly optimised at JET where the plasmas pressure and q-profiles are controlled during the initial current ramp-up phase of the discharge [24]. This regime of operation briefly described in this paragraph is called the "Optimised Shear" regime.

The scenario usually starts with the application of the Lower Hybrid (LH) power (typically 1MW during 1s) to ensure a reliable and reproducible plasma breakdown and to already increase the electron temperature in order to slow down the current diffusion. The plasma current is ramped-up at a rate of typically 0.4MA/s with a lower single null X-point magnetic configuration formed after the plasma breakdown during the low power phase (typically 1.5s after the plasma breakdown). Then, between 1MW and 2MW of ICRH (Ion Cyclotron Resonance Heating) powers are applied using hydrogen minority heating scheme with the resonance located near the plasma centre. During this low applied power phase called "pre-heating", the central electron temperature rises up to 6keV while the electron density, n_e, is kept at relatively low values ($n_e \leq 1.5x10^{19}m^{-3}$). The pre-heating phase is finished with the application of the full powers required to trigger a transition into a plasma state with reduced transport coefficients: up to 18MW of NBI (Neutral Beam Injection) powers combined with 6MW of ICRH powers. As shown on Fig. 1a the central density, n_{eo}, and ion temperature, T_{io}, are rising sharply after the application of the full additional heating power, indicating a change in the particle and energy confinement. In this precise case, the ITB is triggered at t=5.4s while keeping an L-mode condition at the plasma boundary. The phase with an L-mode edge lasts 1.3s after the ITB formation until t = 6.7s when precisely a transition to an ELM-free H-mode occurs spontaneously. Subsequently, as shown on the time trace of the neutron rate production (Fig. 1a) several large ELMs terminate the phase of high performance.

As already pointed out in the introduction of this paper, another approach consists in the combination of an ITB with a weaker edge pressure pedestal of the ELMy H-mode. A Typical time evolution of such discharge is shown on Fig. 1b where both the ITB and the ELMy H-mode are triggered practically simultaneously (The ITB is triggered at t=6s). The ELMy H-mode sequence is characterised on the D_α emission signal by ELMs of medium amplitude at high frequency.

In order to successfully trigger an ITB a minimum amount of additional power has to be applied during the plasma current ramp-up phase. To better quantify this power level, the thermal ion pressure measured at the plasma core is plotted versus the total injected power (the sum of the ICRH and NBI powers) for discharges of the "Optimised Shear" database. Apart from the applied power the other macroscopic plasma parameters are practically the same, e.g. the toroidal

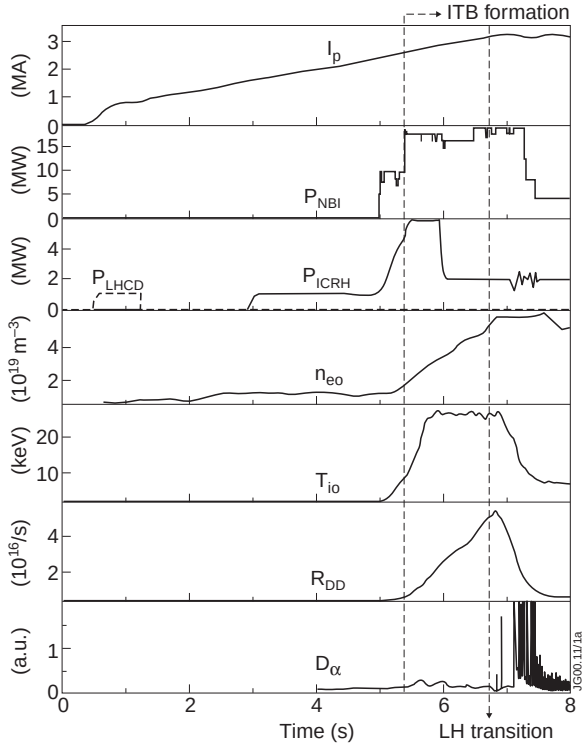

Fig.1a: Time evolution of the plasma current (I_p), additional heating powers (P_{NBI}, P_{LHCD}, P_{ICRH}) central electron density (n_{eo}), the central ion temperatures (T_{io}), the D-D fusion rate (R_{D-D}) and the D_α emission signal. Typical JET "Optimised Shear" discharge where the ITB is triggered during an L-mode (pulse No. 40847).

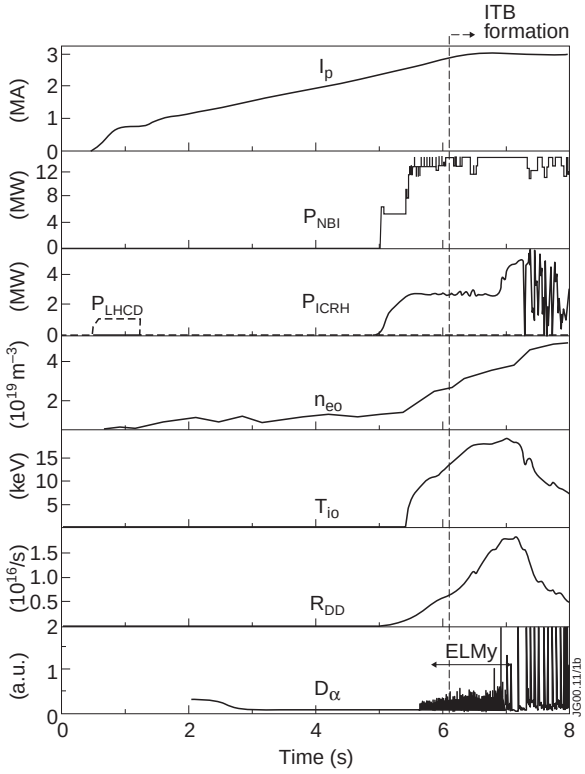

Fig.1b: Time evolution of the plasma current (I_p), additional heating powers (P_{NBI}, P_{ICRH}) central electron density (n_{eo}), the central ion temperatures (T_{io}), the D-D fusion rate (R_{D-D}) and the D_α emission signal. JET "Optimised Shear" discharge where the ITB is triggered during an ELMy H-mode (pulse No. 40038).

fields on axis (B_o) are in the range of 3.4-3.8T, the plasma currents (I_p) of 3.4-3.8MA, the safety factor values close to the plasma edge (at 95% of the poloidal flux) are between 3.5 and 4 with an X-point magnetic configuration. On this figure, discharges with an L-mode and ELMy H-mode edge are separated and respectively identified by open triangles and full circles. When the applied power is increased up to a level of typically 15MW the central pressure smoothly rises up to a value of 0.25×10^5 Pa as expected for the low confinement regime. Slightly above this power level, conditions have been found where the central ion pressures could abruptly rise by a factor ten (up to 2.5×10^5Pa) indicating a change in the core confinement, i.e. formation of an ITB.

Nevertheless, the power level estimated around 15MW is not a sufficient control parameter to guarantee the formation of an ITB. Indeed, as shown on Fig. 2 the confinement properties of some discharges where the applied power is above 15MW could follow a low confinement branch, i.e. keeping a relatively low central pressures even at high power (c.f. the experimental point between 15MW and 25MW with a central pressure below 0.5×10^5Pa). More precisely, it will be shown in sections four and five that the plasma profiles (safety and pressure profiles) at the time of the application of the high power play a major role in the conditions to trigger an ITB.

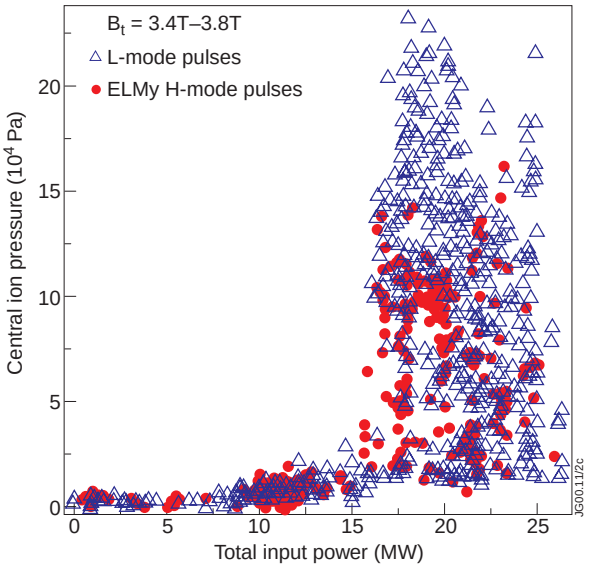

Fig.2: Central ion pressure versus the total input power for discharges with either an L-mode (open triangles) or ELMy H-mode (full circles) edge.

Finally, it is worth mentioning that this figure also illustrates the difference in core performances between discharges with an L and an ELMy H-mode edge. The peak performances are recorded in operation with an L-mode edge with a core ion pressure rising up to 2.5×10^5Pa. Discharges combining an ITB with an ELMy H-mode have reached a significantly lower value of central ion pressures, i.e. up to 1.6×10^5Pa in the best cases. As it will be quantitatively discussed in section 5, the edge conditions (L-mode or H-mode edge) affect the quality of the ITBs (e.g. by reducing the core pressure gradient) and in turn affect the core performances.

3. CHARACTERISATION OF THE TEMPERATURES PROFILES EVOLUTION AND GLOBAL CONFINEMENT IN OPTIMISED SHEAR REGIME

In this section, the radial location of the ITB is estimated by a systematic determination of the region with steep gradients in the ion and electron temperature profiles. The method of analysis of the radial profiles is explained in the first sub-section and is applied to the discharges of the "Optimised Shear" database to study the radial expansion process of the ITBs. Then, the relationship between the radial location of the ITBs and the improved confinement factors is discussed.

In all the analyses presented in this paper, the electron temperature profile, T_e, are measured with the Electron Cyclotron Emission (ECE) diagnostic using a heterodyne radiometer technique. Among the diagnostics used at JET to measure the electron temperature, the ECE diagnostic has been chosen for this work due to its high space resolution (routinely 2cm) which is well suited to study the physics of transport barrier. For the ECE measurements the time resolution could be as low as 8μs, but in our reduced database the T_e-profiles have been stored only at the times of measurement of the ion temperatures profiles. The absolute error on the T_e-profiles is of about 10% but the relative error between the different observation radii is reduced down to 2%. The ion temperature profiles are measured with the charge exchange spectroscopy diagnostic that has a radial and time resolution of respectively 10cm and 10ms. Typical time evolution of the electrons and ions temperature profiles is shown on Figures 3a and 3b for a discharge where an ITB is formed 0.3s after the application of the high power. On JET, internal transport barriers are triggered by mainly using ion heating methods (NBI heating) which partly explains why the ion

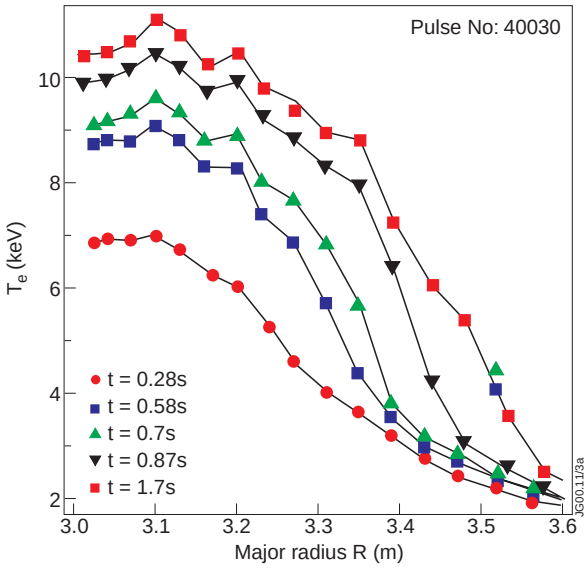

Fig.3a: Time evolution of the electron temperature profiles (pulse No. 40030). Time refers to start of main heating phase (5.4s). T_e-profiles are measured with the ECE heterodyne radiometer diagnostic.

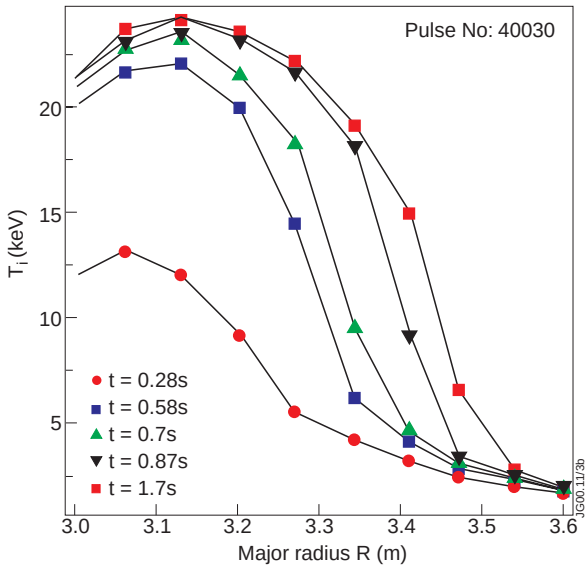

Fig.3b: Time evolution of the ion temperature profiles (pulse No. 40030). Time refers to the start of the main heating phase (5.4s). T_i-profiles are measured with the charge-exchange spectroscopy diagnostic.

temperature is generally larger then the electron one (as illustrated on the Fig. 3 where T_{io}=24 keV and T_{eo}=11 keV at the peak performance time).

3.1. Radial location of the internal transport barriers

Steep gradients, ∇T, in the ion and electron temperature profiles are indicative of a reduction of the anomalous transport, i.e. formation of an ITB. The thermal diffusivity coefficients, χ , are significantly reduced when at a given radial position there is an abrupt change of the temperature gradients. Indeed, the local heat flux, $\Gamma(r) = n \chi \nabla T$, across a given magnetic surface r, is a continuous function of the plasma radius. Consequently, a radial discontinuity in the temperature gradients is indicative of the sudden reduction of the thermal transport coefficients. In other words, the position of the transport barrier is located at the plasma radius where the largest radial variation of the temperature gradients occurs.

Therefore, the approach used to determine in a systematic manner the location of the ITBs with the same criteria for the large number of discharges of our database consists first in the calculation of the second radial derivative of the temperature profiles (d^2T/dr^2). Then, the locations of the maximum and minimum of the radial derivative of the temperature gradients will respectively indicate the outer foot point of the steep gradient zone, R_{Out} (called R_{ITB} by convention) and the inner point, R_{In}. To avoid spurious determination of R_{In} and R_{Out} associated to the experimental noise on the measured data, the raw signals are filtered with a biorthogonal decomposition method (or singular value decomposition) by keeping the first dominant eigenmodes of the decomposition [25]. Then, the filtered temperature profiles are interpolated on a finer grid than the experimental one using a cubic Spline algorithm. The radial derivatives

are all done on the fixed mathematical radial grid. Finally, the positions of the maxima/minima of d^2T/dr^2 located on the mathematical grid are projected onto the experimental radial grid.

The results of such approach are well illustrated by the concrete example shown on Fig. 4, where both the ion temperature profile and its second radial derivatives are plotted 1.2.s after the ITBs formation. In this precise case, R_{In} and R_{ITB} have been numerically estimated to respectively 3.36m and 3.53m while the position of the magnetic axis is at 3.05m.

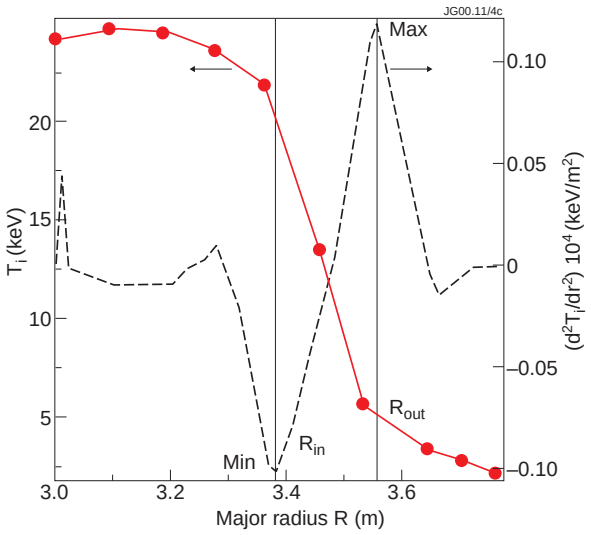

Fig.4: Radial ion temperature profile and its second derivative versus the major radius, (pulse No. 40554). The radial position of the mimum and maximum of d^2T_i/dr^2 allow to determine R_{In} and R_{Out} (also designed by R_{ITB}) as explained in section III-1 of the text.

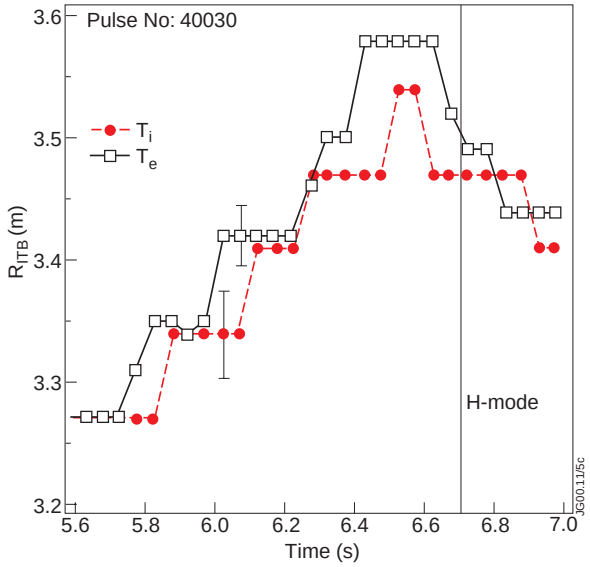

Fig.5: Time evolution of R_{ITB} determined by using either the ion (full circles) or electron (full squares) temperature profiles, (pulse No. 40030). The charge exchange spectroscopy and the ECE diagnostics have been used respectively for the ion and electron temperatures measurements.

Similarly, the method could be used to track the time evolution of the outer foot point of the ITBs. The two evolutions of R_{ITB} determined by using either the ion (full circles) or electron (full squares) temperature profiles measurements are shown on Fig. 5 (the temperatures profiles of the same pulse are plotted on Fig. 3). The ITB is formed inside the plasma core at a radius of 3.28m at a time t = 5.7s with an L-mode edge. The L-mode edge condition is maintained during 1s until t = 6.7s where a transition into an ELM-free H-mode is recorded. The time evolution of R_{ITB} determined from the T_e-profiles consists in three main phases:

(i) a slow outwards expansion of R_{ITB} from 3.28 up to 3.6m which lasts 0.7s at an average velocity ($\Delta R_{ITB}/\Delta t$) of the order of 0.4m/s,

(ii) a short stationary phase where R_{ITB} is maintained at values above 3.5m during 0.3s from t=6.4s up to t =6.7s,

(iii) an inwards contraction process of R_{ITB} which occurs just after the transition into an ELM-free H-mode.

A similar time evolution is also recorded on the R_{ITB} deduced from the T_i profiles. It is worth mentioning that, the sudden variations of R_{ITB} between two consecutive times (i.e., the stair-like shape of the time traces of R_{ITB}) come from the discrete space and time resolution of the temperature profile diagnostics.

The same type of analysis has been repeated for a large number of discharges taken in the "Optimised Shear" database and the results are summarised on Fig. 6. On this figure, R_{ITB} deduced independently from the electron and ion temperature profiles are plotted versus each other for experiments performed with pure Deuterium (full circles) and mixture of Deuterium-Tritium gases (full triangles). It is interesting to point out that the similar values of R_{ITB} is recorded for the D-D and D-T discharges. Nevertheless, Fig. 6 shows that the radial excursion of R_{ITB} is reduced in the pure D-T case (R_{ITB} evolves between 3.4m and 3.55m) compared to the pure D-D case where R_{ITB} is between 3.25m and 3.65m. Finally, Fig. 6 confirms for a larger number of discharges the conclusion drawn from the analysis of Fig. 5 : in both D-D and D-T experiments, the development of steep temperature gradients follows the same time evolution (i.e. formation, expansion and contraction) at the same radial location for both the ion and electron components.

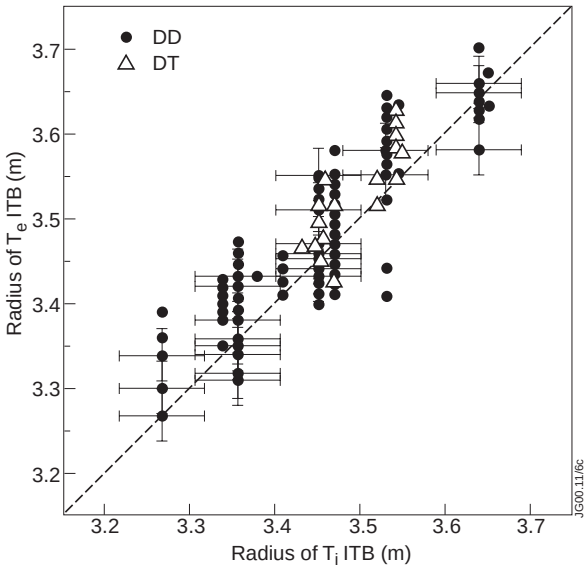

Fig.6: Radial location of the electron ITB against the radial location of the ion ITB for a large number of D-D (full circles) and D-T (full triangles) discharges. The charge exchange spectroscopy and the ECE diagnostics have been used respectively for the ion and electron temperatures measurements.

It is worth pointing out, that different type of R_{ITB} evolution is observed depending on whether the ITBs are triggered with an L-mode edge or in conjunction with an ELMy H-mode regime. This difference is illustrated by the Fig.7 where the evolution of R_{ITB} is plotted for two similar discharges but the edge conditions. The main difference is in the potentiality of the regime which combines an ITB with an ELMy edge to maintain R_{ITB} at steady values after the radial expansion phase. The decrease of R_{ITB} starting at t=6.6s on the time trace labelled by the open triangles on Fig. 7 is generally not observed in the "Double Barrier" mode (full circles). The ITB contraction phase starts at the

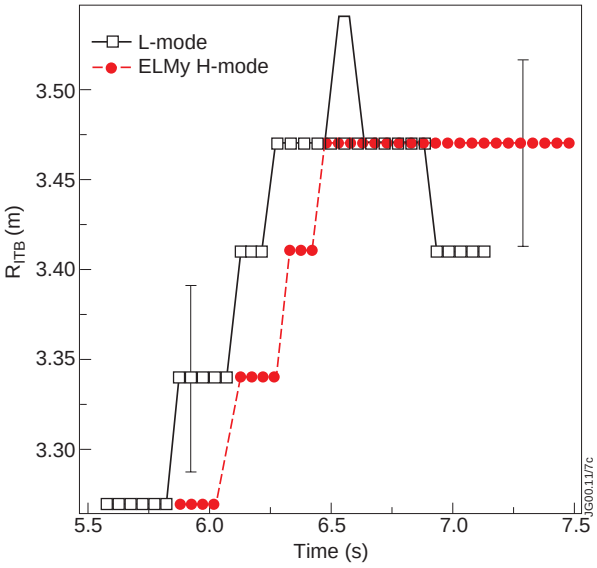

Fig.7: Time evolution of the radial location of the ion ITB (R_{ITB}) for discharges with either an L-mode (open triangles, pulse No. 40030) or an ELMy H-mode edge (full circles, pulse No. 40038).

time of the sudden changes in the edge conditions from an L to an ELM-free regime (t=6.65s). The experimental conditions required to combine simultaneously two transport barriers at different radial location, i.e. at the edge and core of the plasma torus will be further discussed in section 5.

3.2. Global confinement characteristics of the "Optimised Shear" regime

As we could expect from qualitative arguments, the radial location of the ITB directly affects the confinement and the MHD stability properties of the "Optimised Shear" discharges. These links are quantitatively study in this sub-section through the relationship between R_{ITB} and the global performances characteristics assessed in terms of improved confinement factor and normalised beta.

The energy confinement time, $\tau_{E,}$ is directly inferred from the measurement of the global energy content with the diamagnetic loops. The quality of the plasma confinement is assessed by normalising, τ_E, to the standard ITER89-P L-mode scaling prediction [26], $\tau_{ITER89\text{-}P}$: $H_{89} = \tau_E / \tau_{ITER89\text{-}P}$. H_{89} is generally called the improved confinement factor when its value exceeds unity. A non-thermal scaling law has been used to study a large number of discharges since the experimental measurements of the plasma energy is directly the sum of both the thermal and non-thermal energy content. The improved confinement factor, H_{89}, is plotted on Fig. 8 versus R_{ITB} as defined in the previous sub-section. Since the confinement time is normalised to an L-mode scaling law, we have selected the time slices of the discharges where the ITB is combined with an L-mode edge. Hence, the effect of the core performances on the global confinement properties is better revealed. Fig. 8 clearly shows that as the ITB propagates in the outer part of the plasma column, the improved confinement factor rises. The core confinement improvement is sufficient to enhance the global energy confinement time remarkably above the standard L-mode scaling laws. Indeed, H_{89}-factors in the range of 2-2.5 have been obtained at JET when the radial location of the transport barrier is typically at two third of the plasma radius (R=3.6-3.65m) while keeping an L-mode edge.

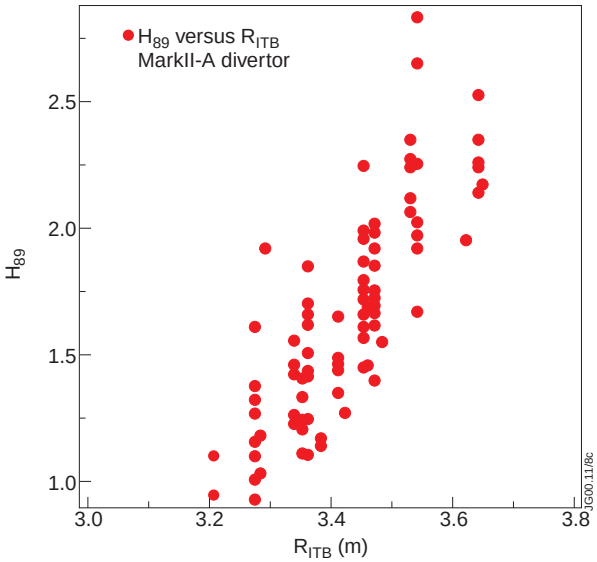

Fig.8: The enhanced energy confinement factor, H_{89}, versus the radial location of the ion ITB for discharges with an L-mode edge.

The global performances and the stability of the discharges are also characterised by the normalised toroidal beta, β_N, defined as $\beta_N = \beta_t /(aB_o/I_p)$ [β_t is the ratio of the volume averaged plasma pressure divided by the magnetic pressure of the toroidal field, a the minor radius]. In fact, the improvement of the plasmas performances to reach steady-sate operation requires increasing simultaneously the H and β_N -factors. The H_{89}-factors are plotted versus β_N values for

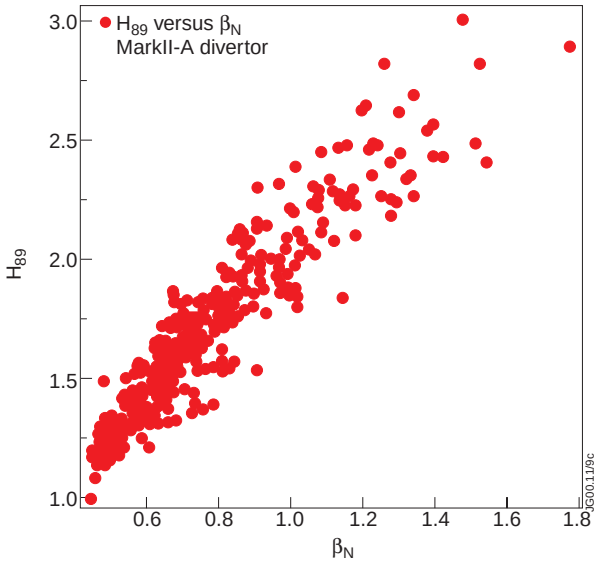

Fig.9: The enhanced energy confinement factor, H_{89}, versus the normalised beta factor, β_N, for a large number of "Optimised Shear " pulses with an L or H-mode edge.

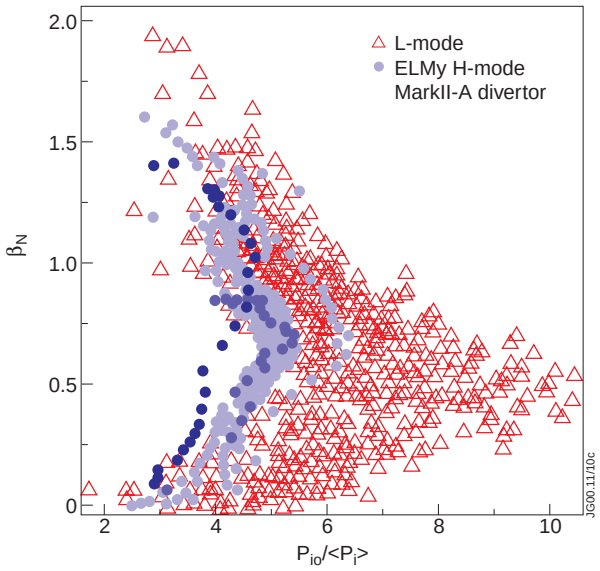

Fig.10: β_N versus the ion pressure peaking factor for discharges with an L-mode edge (open triangles) and ELMy H-mode (full circles).

discharges with either an L or an H-mode edge. When the H_{89}-factors reach values of almost 3, the normalised toroidal betas stay bellow 2. A major difficulty consists in increasing the β_N values while keeping an MHD stable operation in the "Optimised Shear" regime which is characterised by broad current density profiles with low internal inductance (l_i). Ideal MHD stability calculation of the long wavelength kink pressure driven mode has predicted that a broad pressure profile could result in an increase of the observed β_N limit [27-28]. Therefore an operational diagram of practical interest consists in the plot of β_N versus the ion pressure peaking factor, $P_{io}/\langle P_i\rangle$, (central ion pressure divided by the volume averaged ion pressure profile) as drawn on Fig. 10 for a large number of discharges. The ion pressure profile peaking factor is directly deduced from the measurements carried out with the charge exchange spectroscopy diagnostic and is a good indication of the total pressure peaking in these dominant ion heating experiments. In the β_N - $P_{io}/\langle P_i\rangle$ plane, the "Optimised Shear "discharges with an L-mode edge (open triangles) follow the trajectories described hereafter :

(i) initially the discharges start at low β_N and low pressure peaking factor;

(ii) when the high power is applied and the ITB builds up in the core plasma, the pressure peaking factor rises while β_N is still relatively low, i.e. $P_{io}/\langle P_i\rangle$ reaches values up to 10 while β_N is close to 0.6 with an L-mode edge;

(iii) then the radial expansion of the ITB and ultimately the L to H transition naturally broaden the pressure profiles, i.e. β_N rises typically up to two with a pressure peaking factor of 4.

Discharges where an ITB is triggered simultaneously with an ELMy H–mode are identified on the same figure by the full circles. In this case the edge conditions insure that a broader (i.e., $P_{io}/\langle P_i\rangle$ values does not exceed 6 in this case) and therefore a more stable pressure profiles are maintained even during the initial phase of the ITB formation. During the broadening of the

pressure profile β_N is approximately kept below the following curve, $\beta_N \leq 6 / P_{io}/\langle P_i \rangle$, empirically deduced from this database analysis. Above this limit, discharges generally disrupt due to the unstable n=1 ideal pressure driven kink MHD mode [28]. In order to avoid this disruptive zone, it is worth mentioning that the additional heating powers (NBI and/or ICRH) are generally feedback controlled in real-time on a pre-programmed waveform of signal containing information on the plasma pressure and peaking factor [24].

4. SAFETY FACTOR PROFILES AND INTERNAL TRANSPORT BARRIERS

In our present database the safety factor profiles, q, are deduced from the magnetic reconstruction code (EFIT) constrained by the measurements of the magnetic probes located on the JET vessel. Indeed, the motional Stark Effect (MSE) diagnostic generally used to better determine the q-profile especially in the plasma core was not yet installed at JET for the experiments described in this paper. As an example, two typical q-profiles of "Optimised Shear" discharges with respectively an ELMy H-mode and L-mode edge are plotted on Fig 11. Profiles have been produced one second after the main heating phase starts when the ITBs are already formed. The importance of the error bars of the q profiles in the inner half plasma radius makes difficult a conclusion on the exact shape of the q profiles. Nevertheless, the present reconstruction indicates that the q-profile is monotonic with a weak magnetic shear in the plasma core. The trend is that "Optimised Shear" discharges with an ELMy H-mode edge has a weaker magnetic shear already at mid-plasma radius compared to the same discharge but with an L-mode edge. This trend is explained qualitatively by an expected higher bootstrap current at the plasma periphery due to the edge pressure pedestal. Typically, "Optimised Shear" pulses with an L-mode edge have an internal inductance, l_i, of 0.8 compared to 0.7 with an ELMy H-mode edge indicating also the formation of a broader current density profile when an edge transport barrier is present.

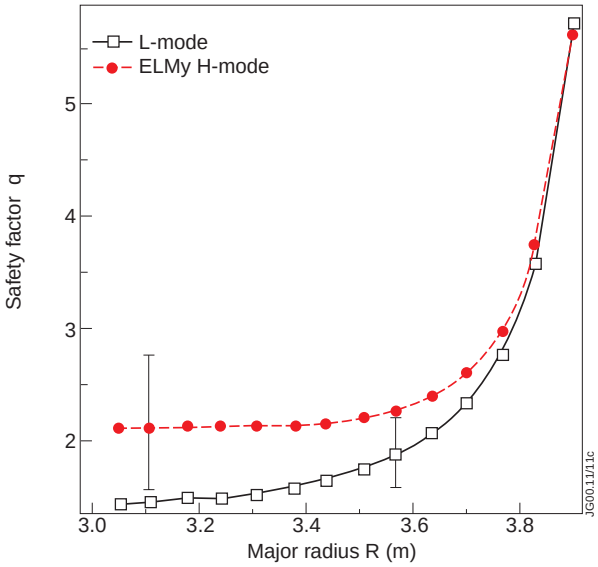

Fig.11: q-profiles deduced from the magnetic reconstruction code, EFIT, of two "Optimised Shear" discharges with either an L-mode (open triangle, pulse No. 40030) or an ELMy H-mode edge (full circles, pulse No. 40038). The q-profiles are shown one second after the start of the main heating phase.

Despite the large error bar on the q-profile, we propose to study the link between the q-profiles and the ITB locations. In the database, the q-profiles are characterised either by their values or their local magnetic shear at R_{ITB} (the method used to determine R_{ITB} has been described in section three). For a given pulse, the time evolution of the ITB radii determined on the electron

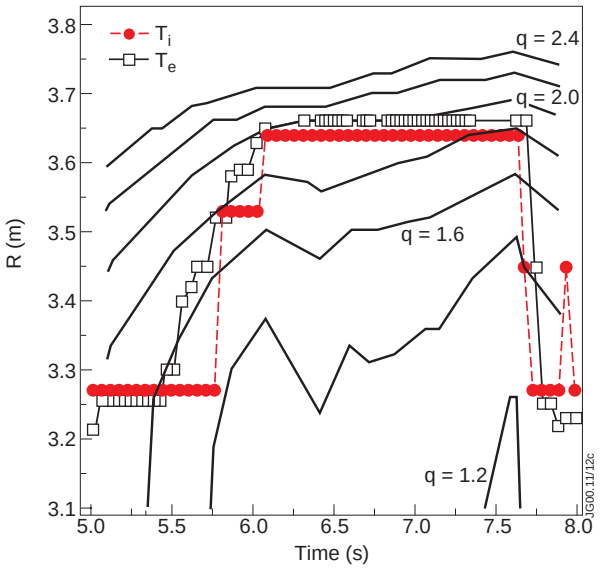

Fig.12: Time evolution of R_{ITB} deduced either from the T_i (full circles) or T_e (full squares) profiles together with the contour lines of the q-profile (pulse No. 40542). The transition to an ELMy H-mode occurs at t=6.1s.

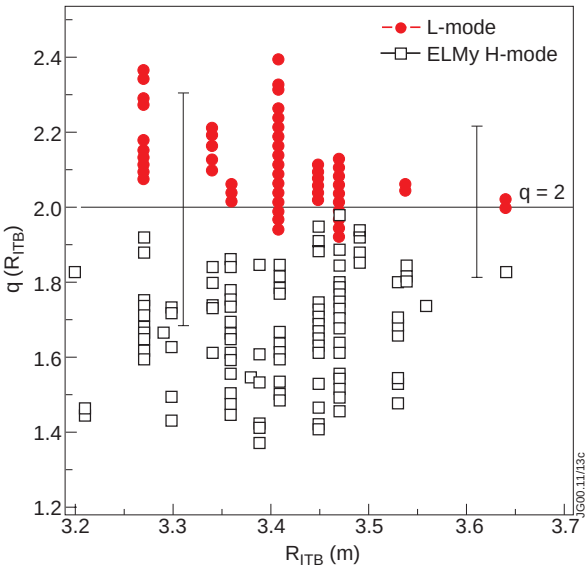

Fig.13: Values of the safety factor at the radial position of the ion ITB, $q(R_{ITB})$, against R_{ITB} for discharges with either an L-mode (open triangles) or an ELMy (full circles) H-mode edge.

(full squares) and ion (full circles) temperature profiles are plotted on Fig.12 together with the time evolution of the radii of constant q-values. This pulse has an ITB triggered with an L-mode edge and the transition into an ELMy edge occurs at t=6.1s. The ITB is formed inside the rational q=2 surface and expands radially up to the q=2 surface. We notice also that the expansion of the ITB occurs on a faster time scale than the slow evolution of the q-profile. Figure 13 is a plot of the safety factor values at the ITB radii, R_{ITB}, versus R_{ITB} for several discharges with either an ELMy H-mode or an L-mode edge. The global trend observed in this figure is that the ITBs are located close to the q=2±20% surface. One can observe that all discharges with an L-mode edge have q values at the outer foot point of the transport barrier, $q(R_{ITB})$ just bellow q=2. As far as the ELMy H-mode discharges (black circles) are concerned, the $q(R_{ITB})$ values are generally slightly above q=2. Finally, for the same set of discharges the local magnetic shear calculatedat R_{ITB} has been represented versus R_{ITB} (Fig. 14). The magnetic shear at the ITB radius varies from 0 to 1.5 while the ITB expands from R=3.2m to R=3.65m in the L-mode discharges. For the ELMy discharges the magnetic shear values at the ITB radii are within a range of 0 to 0.5. As shown by Fig. 13 and 14, ITBs are formed in the region of low

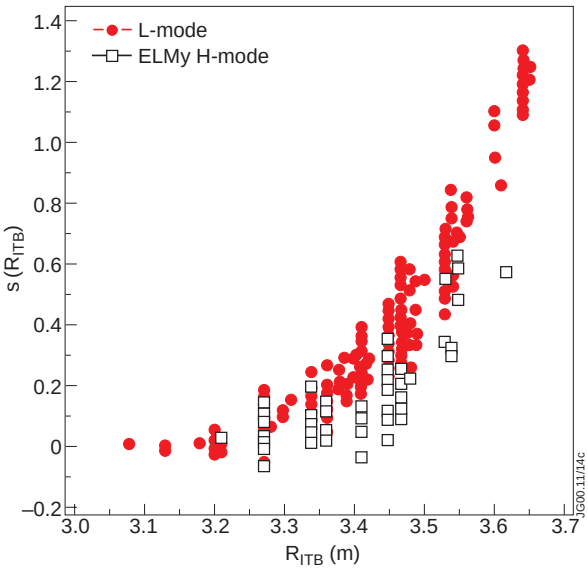

Fig.14: Magnetic shear at R_{ITB} versus R_{ITB} for discharges with either a L-mode (open triangles) or ELMy (full squares) H-mode edge.

magnetic shear inside the q=2 surface [28]. Fig. 14 clearly illustrates that the internal transport barriers are not necessary confined to a zone of low magnetic shear and propagate to regions where magnetic shear is strongly positive (up to s=1.5 for L-mode discharges).

5. **EDGE CONFINEMENT AND INTERNAL TRANSPORT BARRIERS**

The conditions to successfully combine two transport barriers located at the plasma core and edge are discussed in this last section before the final conclusion. It has already been shown (c.f. Fig.5 for instance) that the radial location of the ITB moves towards the plasma centre in conjunction to the build-up of the edge pressure pedestal during the ELM-free phase after the H-mode is triggered.

To further analyse the coupled dynamics of the two transports barriers, we first quantitatively define simple criteria, to assess the "quality" of the transports barriers in terms of confinement reduction, which could be applied to the whole "Optimised Shear " database. For the core physics, the quality of the confinement inside the ITB is evaluated by calculating the inverse of the local ion temperature scale length, L_{Ti}^{-1}, defined by the following expressions:

$$L_{TI}^{-1} = \frac{|\nabla Ti|}{T_m}$$

where

$$|\nabla Ti| = \left| \frac{Ti(R_{Out}) - Ti(R_{In})}{R_{Out} - R_{In}} \right| \quad \text{and} \quad T_m = [T_i(R_{In}) + T_i(R_{Out})]/2$$

T_m and $|\nabla T_i|$ are respectively the radial averaged ion temperature and its gradient between R_{In} and R_{Out}. For the sake of simplicity, the ion temperature profiles (T_i) have been used in our study to calculate L_{Ti}^{-1}, since in these dominant ion heating experiments the "quality" of the ITBs is clearly revealed on the T_i-profiles. As far as the edge physics is concerned, we have chosen to characterise the quality of the edge confinement by the values of the ion temperature measured on the most external line of sight of the charge exchange spectroscopy diagnostic, i.e. R=3.74m, called $T_{i\text{-edge}}$.

The interplay between the two transport barriers, i.e. how the core confinement is affected by the edge conditions, is studied in an original diagram where L_{Ti}^{-1} characterising the core steepness of the T_i -profiles are plotted versus the edge ion temperatures, $T_{i\text{-edge}}$ (c.f. Fig. 15a and 15b). This representation is convenient to analyse a large number of pulses of the "Optimised Shear" database with different edge conditions and edge confinement, i.e. L-mode edge, ELMy H-mode with type I and Type III ELMs and ELM-free H-mode. Indeed, Figs 15 shows that $T_{i\text{-edge}}$ is found to vary from 0.5keV with a L-mode edge up to 8keV after a long ELM free H–mode phase.

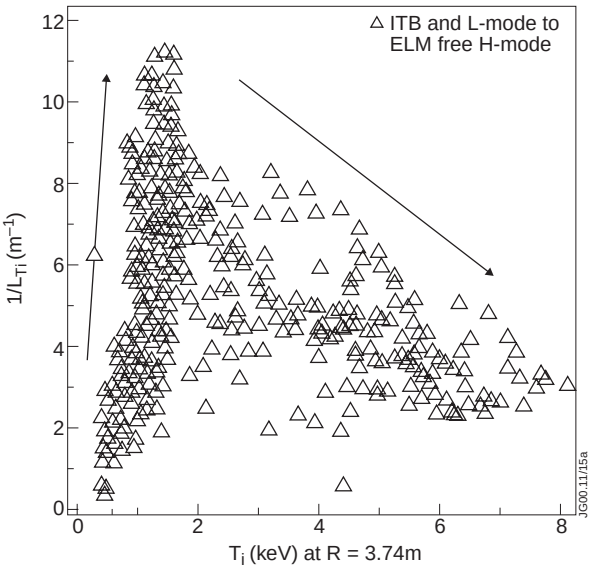

Fig.15a: Inverse scale length of the ion temperature gradient, L_{Ti}^{-1}, versus the ion temperature measured at the plasma periphery, R=3.74m. The sub-set of discharges selected for this diagram corresponds to the case where the ITBs are triggered and radially expanded with an L-mode edge before the transition into an ELM-free H-mode.

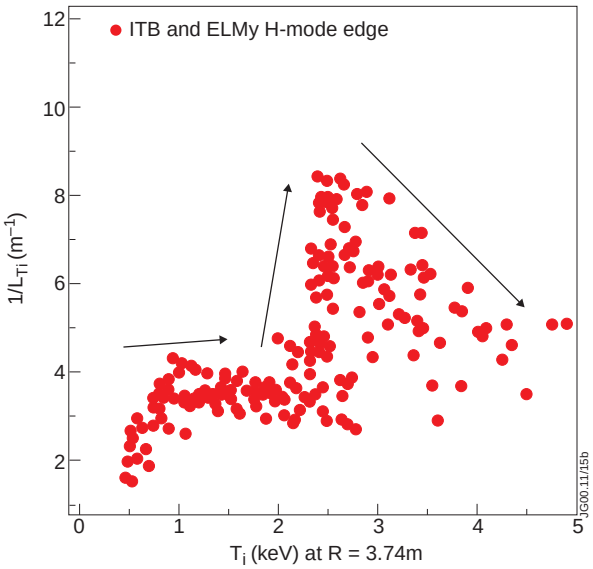

Fig.15b: Inverse scale length of the ion temperature gradient, L_{Ti}^{-1}, versus the ion temperature measured at R=3.74m. The sub-set of discharges selected for this diagram corresponds to the case where the ITBs are triggered simultaneously with an ELMy H-mode edge.

On Fig. 15a, we have selected discharges where the ITBs are triggered and expand radially before the transition into an ELM-free H-mode occurs. In this diagram the build-up of the internal barrier with an L-mode edge, i.e. L_{Ti}^{-1} rises from $1m^{-1}$ up to $12m^{-1}$, is produced at a practically constant $T_{i\text{-edge}}$ ranging from 1.5keV up to 2keV (Fig. 15a). When the transition into an ELM-free H-mode occurs, the edge temperature rises while simultaneously the quality of the internal barrier deteriorates. Fig. 15a shows that on average on the pulses of our database, L_{Ti}^{-1} decreases from $12m^{-1}$ to $3m^{-1}$ when $T_{i\text{-edge}}$ increases from 2 keV up to 8 keV. The degradation of the ITB quality, as revealed from this representation, seems to be correlated with the improvement of the edge confinement, i.e. formation of the edge transport barrier. During the ELM-free H-mode phase, the combination of the internal and external barrier is transient (cf. Fig. 5 for the time evolution) and the ITBs could not be sustained.

The same type of operational diagram has been drawn for discharges where ITBs are triggered simultaneously in combination with an ELMy H-mode edge (Fig. 15b). The continuous ELMs prevent the build-up of the pressure pedestal in contrast to the ELM-free H-mode and $T_{i\text{-edge}}$ is limited up to 4.5keV for these discharges. This figure indicates that steep temperature gradients with L_{Ti}^{-1} up to $8.5m^{-1}$, could be sustained together with an ELMy H-mode when the edge temperature is maintained between 2.5keV and 3.5keV. Above these $T_{i\text{-edge}}$ values, we recover the degradation of the core performances as observed with an ELM-free H mode edge (Fig. 15a). Therefore, our analyses indicate that for steady-state operation a control of the edge

confinement, i.e. control of the edge pressure pedestal, is required to sustain the high core performances. It is worth pointing out, that in the recent ITB experiments performed at JET the edge pressure was controlled by increasing the radiation level thought high-Z impurity (e.g. Argon) injection [30]. With such a control, the simultaneous combination of the ELMy edge with an ITB is a promising route for high performance and steady-state operation with an X-point magnetic configuration.

6. CONCLUSION

Global characteristics of the internal transport barriers physics have been studied in this paper by exploring the large JET "Optimised Shear " database of D-D and D-T discharges realised during the 1996-1997 experimental campaigns [21-22]. The database contains the relevant global and local information for up to 300 experiments performed with the same divertor, "MkIIA", in a lower single null X-point magnetic configuration at a toroidal magnetic field in the range of 3.4-3.8Tesla. For such conditions, it has been shown that the minimum applied power (i.e., a combination of NBI and ICRH powers applied during the ramp-up phase of the discharge) to trigger an ITB should exceed 15MW. Above this power level, ITBs are not systematically produced since the favourable conditions to trigger an ITB depends also on the plasmas profiles (pressure and q-profiles) when the high power is applied. In particular, it was found that a low magnetic shear inside the q=2 surface were favourable conditions to form an ITB.

The temperature profiles of the "Optimised Shear" discharges have been characterised with the same criteria by calculating: (i) the radial location of the foot of the steep gradient region (R_{ITB}), (ii) the width of steep gradient zone (R_{In}) and (iii) the temperature scale length at the ITB location (L_T). These quantities have been deduced from the radial derivatives of the noise-filtered profiles. For all the discharges analysed, the transport barrier is formed close to the magnetic axis, and expands radially towards the plasma periphery. The radial expansion of R_{ITB} across the plasma torus takes place at an average speed of 0.4m/s. During the expansion process, the q-profiles also slowly evolve: in particular, R_{ITB} was found to be close to the position of the q=2 surface. An inward contraction process of the ITB (i.e. reduction of R_{ITB}) is generally observed simultaneously with the change of the edge confinement from L to H mode edge. Furthermore, we have found that the same values of R_{ITB} are identified either on the electron or ion temperature profiles. The positions of the core transport barrier are the same (within the error bars associated to the radial resolution of the diagnostics) for the electron and ion temperatures. The global performances in terms of confinement and MHD stability are strongly linked to the dynamics of the ITB and their radial locations. The improved confinement factor, H_{89}, (the diamagnetic energy confinement time normalised to ITER-89 scaling law) increases with R_{ITB} up to H_{89}=2.5 with an L-mode edge when the ITB is approximately at two third of the plasma radius. The trajectories of the discharges in a plane β_N versus the pressure peaking factor have shown that β_N values have been increased up to two thanks to the broading of the pressure

profile during the expansion process. As far as the global MHD stability is concerned, discharges with an ELMy H-mode edge have on average broader pressure profiles and could stay farther from the unstable MHD domain.

Finally, the interplay and the (non-linear) link between two transport barriers simultaneously located at the core and edge of the plasma have been studied in view of optimising the route towards steady operation. To clarify the analysis, two categories of discharges have been identified depending on the edge conditions (L mode or ELMy H-mode edge) when the ITB is triggered. An original operational diagram has been drawn where the inverse of the ion temperature scale length, L_{Ti}^{-1}, evaluated at R_{ITB} has been plotted versus the edge ion temperature, $T_{i\text{-}edge}$, which characterises the edge temperature pedestal. Steep gradients in the plasma core, with L_{Ti}^{-1} up to $12m^{-1}$, have been produced while keeping an L-mode edge condition. These high performance plasmas could not be sustained more than one or two confinement times. Indeed, after the inevitable transition into an H-mode edge (ELM-free) the core performances are reduced: L_{Ti}^{-1} decreases from $12m^{-1}$ to $3m^{-1}$ when $T_{i\text{-}edge}$ increases from 2 keV up to 8 keV. When an ITB is triggered simultaneously with an ELMy H-mode edge, the core performances could be sustained on longer time scale if the ELMs activity is sufficient to prevent the build-up of the edge temperature. Therefore, the combination of an ITB with an ELMy H-mode edge is a promising route for high performance and steady state operation with an X-point magnetic configuration. Nevertheless, active and integrated plasma controls of the edge temperature simultaneously with the core profiles (pressure and q-profiles) are required to reach and sustain this stable high-confinement regime with two transport barriers.

ACKNOWLEDGEMENTS

It is a pleasure to acknowledge the entire JET team for its strong implication in the success of the experiments described in this paper.

REFERENCES

[1] Taylor, T. S., Plasma Phys. Control. Fusion 36 (1997) B229.

[2] Gormezano, C., et al, Plasma Phys. Control. Fusion 40 (1998) A171.

[3] Litaudon, X., Plasma Phys. Control. Fusion 40 (1998) A251.

[4] Kessel, C., *et al*, Phys. Rev. Lett. 72 (1994) 1212.

[5] Wolf, R.C, et al, invited paper at the 26th EPS Conf. On Controlled Fusion and Plasma Physics, Maastricht, 1999. To appear in Plasma Phys. Control. Fusion.

[6] Strait, E.J, *et al*, Phys. Rev. Lett. **75** (1995) 4421.

[7] Tuccillo A. A. et al. Applications of Radio-frequency Power to Plasmas (Proc. 12th Top. Conf. Savannah Georgia 1997), American Institute of Physics, New York, (1997) p. 121.

[8] Gormezano, C., and JET Team, in Fusion Energy 1996 (Proc.16th Int. Conf. Montreal, 1996), Vol. 1, IAEA, Vienna (1997) p. 487.

[9] Ishida, S., et al Phys. Rev. Lett. **79** (1997) 3917
[10] Fujita, T., et al, Phys. Rev. Lett. **78** (1997) 2377.
[11] Lopes Cardozo N.J., et al, Plasma Phys. Control. Fusion **39** (1997) B303.
[12] Levinton F.M, *et al*, Phys. Rev. Lett. **75** (1995) 4417.
[13] Equipe Tore Supra, Plasma Phys. Control. Fusion **38** (1996) A251.
[14] Hoang G.T., et al, in Controlled Fusion and Plasma Physics (Proc. 26th Eur. Conf., Maastricht 1999) vol23J, European Physical Society, Geneva, (1999) p. 105.
[15] Söldner F.X. and the JET Team, Plasma Phys. Control. Fusion **39** (1997) B353.[16] Gormezano C., *et al*, Phys. Rev. Lett. **80** (1998) 5544.
[17] Litaudon X., et al, Plasma Phys. Control. Fusion **41** (1999) A733.
[18] Ide S., Fujita T., Naito O., Seki M. Plasma Phys. Control. Fusion **38** (1996) 1645.
[19] Litaudon X., *et al*, Plasma Phys. Control. Fusion (1996) **38** 1603.
[20] Barbato E., et al, Controlled Fusion and Plasma Physics (Proc. 24th Eur. Conf. Berchtesgaden 1997) vol 21A, European Physical Society, Geneva, (1997) p1161.
[21] Keilhacker,M., et al Nucl. Fusion 39 (1999) 209.
[22] Jacquinot, J., et al Nucl. Fusion 39 (1999) 235.
[23] Söldner F.X., *et al*, Nucl. Fusion **39** (1999) 407.[24] Sips A.C.C., *et al*, Plasma Phys. Control. Fusion **40** (1998) 1171.
[25] Dudok de Witt, A.-L. Pecquet et J.C. Vallet, Phys. Plasmas **1** (1994) 3288.
[26] Yushmanov, P.N., Takizuka, T., Riedel, K.S., Kardaun, O.J.W.F., Cordet, J.G., Kaye, S.M., Post, D.E., Nucl. Fusion **30** (1990) 1999.
[27] Lazarus E.A., *et al*, Phys. Rev. Lett. **77** (1996) 2714.
[28] Huysman G., *et al*, in Controlled Fusion and Plasma Physics (Proc. 24th Eur. Conf. Berchtesgaden, 1997), vol 21A, Part I, European Physical Society, Geneva, (1997) p. 21.
[29] Challis C., et al, in Controlled Fusion and Plasma Physics (Proc. 26th Eur. Conf., Maastricht 1999) vol23J, European Physical Society, Geneva, (1999) p69.
[30] Gormezano C. invited paper at the 26th EPS Conf. On Controlled Fusion and Plasma Physics, Maastricht, 1999. To appear in Plasma Phys. Control. Fusion.